Seventh International Conference on Computational Fluid Dynamics (ICCFD7), Big Island, Hawaii, July 9-13, 2012

ICCFD7-1701

Analysis and Optimization of Guide Vane Jets to Decrease the Unsteady Load on Mixed Flow Hydroturbine Runner Blades

B. J. Lewis*, J. M. Cimbala and A. M. Wouden
*Corresponding author: BJL5176@PSU.EDU
The Pennsylvania State University, USA.

Abstract: As the runner blades of a mixed-flow hydroturbine pass through the wakes created from the guide vanes, they experience a significant change in absolute velocity, flow angle, and pressure. The concept of adding water jets to the trailing-edge of the guide vanes is proposed as a method for reducing the dynamic load on the hydroturbine runner blades. Computational experiments show a decrease in velocity variation experienced at the location of the runner blades with the addition of the jets. The decrease in velocity variation should result in a reduction in dynamic load on the runner blades. A simple optimization procedure was performed to determine the optimal jet flow rate to negate the effect of the wake deficit.

Keywords: Hydroturbines, Trailing-Edge Blowing, Turbomachinery, CFD.

1 Introduction

Over the past decade, many countries have experienced a significant increase in alternative electricity generation. In order to maintain stability in the electric power grid, it has become common practice to utilize hydroturbines for load following. This practice requires hydroturbines to operate in conditions far from their design point. The flow through a hydroturbine during off-design operation is highly unsteady, resulting in load variation on the runner blades, flow separation, vibration, and cavitation. The unsteady pressure field caused by the interaction of the guide vane wakes with the runner blades is the omnipresent source of dynamic load on hydroturbine components [1]. As the runner blades pass through these wakes, they experience a significant change in absolute velocity, flow angle, and pressure. Reducing the unsteady load on runner blades would allow for leaner designs, smoother operation, and an increased lifespan of the hydroturbine and generator components.

This paper presents a method for reducing the dynamic load on the runner blades of a Francis turbine by injecting water from the trailing-edge of the guide vanes to compensate for the momentum deficit of the wakes. This method is validated computationally using a steady-state CFD simulation of a single distributor vane passage from a model Francis hydroturbine. The CFD simulations were performed using OpenFOAM®, an open-source CFD software, using a pressure-based finite volume method.

2 Previous Research in Trailing-Edge Blowing

In the early 1960's, Dr. Eduardo Naudasher [2], and his students Ridjanovic [3] and Wang [4], at the Institute of Hydraulic Research of the University of Iowa, began studying the turbulent behavior of flow in the wake of a body with hydrodynamic self-propulsion at high Reynolds numbers. The basic concept of self-propulsion is that the drag on the disturbing body is balanced by a source of added momentum internal to the body. When the added momentum and drag on the body are in balance, a momentumless wake is formed. Experimentally, momentumless wakes are most often achieved by injecting additional fluid from the

trailing-edge of the body. Practical examples of self-propelled bodies are submarines, aircraft, and missiles, when traveling at a constant velocity.

2.1 Basic Research: Axisymmetric and 2-D Cases

Following Naudasher's work [2], significant research, both experimental and computational, has been conducted on trailing-edge blowing and momentumless wakes. Sirviente and Patel [5] analyzed the wake of a slender self-propelled body. The primary focus of the study was to understand the mixing of the two distinct shear layers and their evolution into a single shear layer. Sirviente and Patel [6] also investigated the effect of a swirling jet from the trailing-edge of the slender body and showed that swirl increased the momentumless wake dissipation rate. The effect of swirl in the mean flow on a similar slender self-propelled body was analyzed by Chernykh et al. [7]. They determined that mean flow swirl also improved the wake dissipation rate. As these types of self-propelled bodes are common test cases for ocean vehicles, Brucker and Sarkar [8] also studied their behavior in stratified media.

Cimbala and Park [9, 10] investigated the turbulent structure of 2-D momentumless wakes at moderate Reynolds numbers using various configurations of the trailing-edge jet. Their experiments demonstrated that the decay rate for the centerline velocity difference was much faster for the momentumless wake than for the pure wake. Park and Cimbala [10] also concluded that a jet configuration using two thin slots, equally spaced from the centerline of the body, resulted in a more rapid decay when compared with the single jet centered on the trailing-edge (see Figure 1).

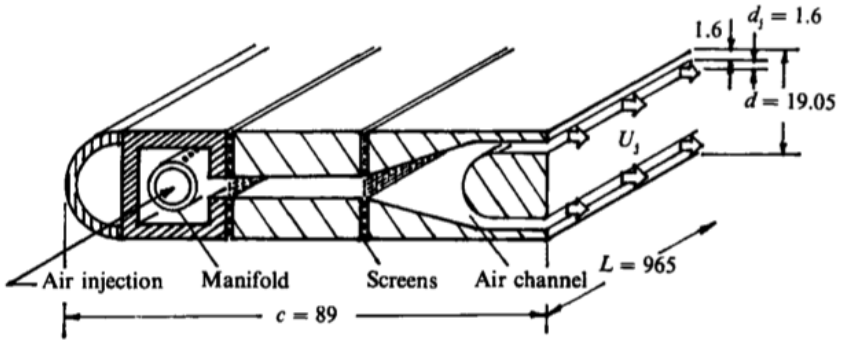

Figure 1: Schematic of the two slot configuration of the 2-D momentumless wake body (dimensions in mm) [10].

Further investigation was then performed by Meyer and Cimbala [11] focusing on wake suppression for finite airfoils, and Corcoran [12] and Naumann [13] who experimented with several blowing techniques. Corcoran [12] showed that trailing-edge blowing reduces Reynolds stress, vorticity, and velocity fluctuations within one chord length downstream. Though an important finding, Francis hydroturbine blades are most often located less than one guide vane length downstream. Naumann [13] examined several different configurations for trailing-edge blowing, including a continuous slit at the trailing-edge, a set of discrete jets, and a set of discrete jets with vortex generators. He determined that a set of discrete jets along the trailing-edge provide the best results.

The first computational efforts to predict the flow in a momentumless wake were performed by Birkhoff and Zarantonello [14]. Using dimensional analysis, and assuming standard linearization, an analytical approximation was developed for the velocity profile far downstream for both 2-D and axisymmetric momentumless wakes. Tennekes and Lumley [15] later applied similar arguments to more generally characterize wakes, jets, and momentumless wakes. Both groups assumed an exponential relation for the wake growth rate and centerline velocity defect. However, the exponent in these relations becomes indeterminate for a zero momentum wake. Additionally, Diamessis et al. [16] developed a similarity scaling law based on extrapolation of experimental data for momentumless wakes in stably stratified media.

Various pure eddy-viscosity models were developed by Ginevskii et al. [17], Gran [18], and Ko [19] using Prandtl's hypothesis and classic mixing length theory. Though eddy-viscosity mixing length models had

been found to accurately predict the mean velocity profile for free-shear flows, each of the above models showed very poor agreement with experimental data by Naudascher [2] and others. Schetz and Stabley [20] proposed a modification to the mean velocity gradient term in Prandtl's model. Kubota [21] also developed a modification of Prandtl's model by retaining the higher-order non-linear terms. Both models produced a significant improvement compared with the previous eddy-viscosity mixing length models.

Gran [18] and Swanson et al. [22] developed one-equation turbulence models for momentumless wakes, which showed only marginal improvement over the eddy-viscosity models by Schetz and Stabley [20] or Kubota [21]. Two-equation, $k-\epsilon$ type, models were developed by Kubota [21] and Hassid [23]. In an effort to simplify the model, Kubota's model neglected the production of turbulent kinetic energy (TKE) by mean shear. Hassid's model did not make this simplification, but incorporated both a velocity scale for the mean flow and for the turbulent quantities. The two modified $k-\epsilon$ models agreed well with experimental data by Naudascher [2] and others.

Up to this point in time, the majority of computational efforts for momentumless wakes were focused on axisymmetric cases. This was primarily motivated by the need to understand the flowfield behind axisymmetric self-propelled bodies such as submarines and missiles [24]. Later, the 2-D momentumless wake experiments of Cimbala and Park [9] were used by Ahn and Sung [25] to validate the $k-\epsilon-\gamma$ model by Cho and Chung [26]. The $k-\epsilon-\gamma$ model is a three-equation model that includes the effect of turbulent intermittency. Though not developed for modeling momentumless wakes, Ahn and Sung [25] found that the enhanced treatment of turbulent intermittency in the $k-\epsilon-\gamma$ model produced significant improvements over the standard $k-\epsilon$ model for locations beyond 30 diameters downstream.

Higher-order turbulence models have also been applied to momentumless wakes. Lewellen et al. [27, 28] and Finson [29] used second-order stress closure models to simulate Naudascher's [2] experiments. Later Shashmin [30] and Korobko and Shashmin [31] applied Reynolds stress closure models. The higher-order stress closure models did not show significant improvement over the two-equation models in predicting the mean flow field. A unique third-order model for momentumless wakes in a linearly stratified medium was developed by Chernykh and Voropayeva [32, 33], which produced favorable improvements over previous models.

Attempts have also been made to model momentumless wakes using spectral methods by Diamessis et al. [34], and direct numerical simulation (DNS) through pseudospectral methods by Orszag and Pao [35] and Metcalfe and Riley [36]. The DNS results demonstrated exceptional agreement with a number of experimental data sets; however, at significant computational cost.

2.2 Applied Research: Turbomachinery Flows

For the present work, the most important application for momentumless wakes and trailing-edge blowing is the reduction of rotor-stator interactions and improvement of turbomachinery performance. Trailing-edge blowing from either the guide vanes or rotor blades has been successfully applied to axial flow turbofans, compressors, and turbines. However, no evidence has been found in the literature of the application of trailing-edge blowing to centrifugal machines or mixed flow devices, such as Francis hydroturbines.

Leitch et al. [37] and Rao et al. [38] studied the complete flow through a simple axial turbofan. They found that the flow into the rotor was made more uniform by using trailing-edge blowing to minimize the shed wakes, thus reducing the unsteady rotor-stator interaction. Waitz et al. [39] used trailing-edge blowing, along with boundary layer suction, on an actual rotor blade. It was determined that wake management using trailing-edge blowing is feasible for high-bypass turbofans. Wo et al. [40] studied flow control of the rotor wake in an axial compressor. They concluded that for a wake momentum of 72% of that of the momentumless wake case, a force amplitude reduction of 25% and 35% was realized for the near-design and high loading cases, respectively. Wu et al. [41] investigated the effects of momentumless wakes in a low pressure axial turbine. The results show that the momentumless wakes made the inlet flow of the rotor more uniform and improved the inlet flow angle of the rotor.

2.3 Applied Research: Turbomachinery Acoustics

Another common application of momentumless wakes is to use trailing-edge blowing to reduce the acoustic disturbances created by turbomachinery blades. The unsteady pressure field caused by the interaction of

the stator and rotor blades not only causes large dynamic variation in load on the rotors, but results in high levels of noise. Reducing the acoustic signature of blade interactions is of obvious interest to aerospace and naval applications. In recent years, the U. S. Department of Energy, the Environmental Protection Agency, and other environmental organizations have also investigated this topic in an effort to reduce the impact of wind turbines and hydrokinetic turbines on the surrounding human and animal populations [42].

Basic proof-of-concept experiments were performed by Sutliff et al. [43] to observe the acoustic interaction of the rotor wakes with the downstream stator blades of a low-speed fan. In this case, the additional fluid was injected from the moving rotor blades, rather than the stators. Meyer and Cimbala [44] investigated the feasibility of using trailing-edge blowing for the reduction of discrete tone noise. Succi [45] also examined techniques to suppress the noise associated with the rotor only (applicable to helicopters and propeller-driven aircraft). Each of the studies in Section 2.2 also addressed acoustical aspects of the rotor-stator interaction. In every case, the addition of blowing from either the rotor or the stater was found to reduce the intensity of the acoustic noise caused by rotor-stator interaction, as well as reduce the unsteady variation in load on the machine components.

3 Validation Case: *Wake of a Self-Propelled Body*

In the near wake of any flow obstruction, self-propelled or not, there is a combined presence of both wall bounded turbulence and free-shear layer turbulence. In order to accurately model the flow in this region, the turbulence model must correctly treat the mechanisms for turbulent transport and production seen in both classes of turbulent flow. Higher-order turbulence models have been developed to properly capture the near-wake region; however, the computational cost is impractical when modeling the flow through an entire hydroturbine.

As shown previously, the data from Naudasher's experiment [2] have served as a common validation case for many simulations of wake-jet combination flows and turbulence models. Naudasher's data were also used here to validate the applicability of the standard $k - \epsilon$ turbulence model for predicting the wake of a hydroturbine guide vane with trailing-edge blowing.

3.1 Computational Background

The test apparatus used by Naudasher consists of an axisymmetric disk, mounted on a hollow sting (see Figure 2). The disk was suspended in an octagonal wind tunnel, and air was passed over the apparatus at 60.0 ft/s (18.288 m/s). High pressure air was also supplied to the hollow sting and exited the center of the disk at 218.4 ft/s (66.568 m/s) to create self-propulsion.

A steady-state, axisymmetric, computational simulation of Naudasher's experiments was conducted using OpenFOAM®. The standard high Reynolds number $k - \epsilon$ model was used for turbulent closure. Special consideration was given to the turbulent inlet conditions for the jet. The first approach was to define the jet inlet to be collocated with the trailing-edge of the disk. This approach greatly simplified the grid generation process, and required a smaller cell count. The second approach was to define the jet inlet approximately 20 jet diameters upstream of the disk trailing-edge. This approach more physically incorporates the jet supply channel and it allowed the internal flow field to establish the corresponding exit conditions of the jet. In both cases, a uniform velocity was specified for the entire jet radius. Uniform values for TKE and turbulent dissipation rate were also specified corresponding to the average turbulent conditions of fully-developed pipe flow at the given Reynolds number.

A basic grid resolution study was performed to verify that the solution was grid independent. As shown in Figure 3, the grid was refined four times. Less than a 1% change was observed when the grid was refined from approximately 70,000 to 230,000 cells. However, it is apparent that even further refinement is needed to achieve complete grid independence.

3.2 Results and Conclusions

The resulting wake profiles at various locations downstream of the axisymmetric disk are shown in Figure 4 for both jet inlet approaches. The results clearly demonstrate the necessity of including a portion of the jet supply channel in the computational domain. In addition, including a portion of the jet supply channel is

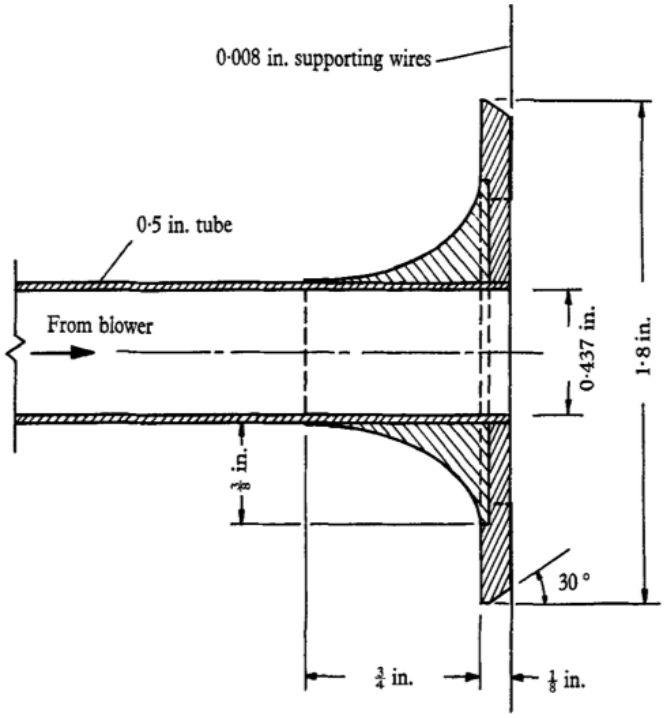

Figure 2: Detailed view of the axisymmetric self-propelled test apparatus [2].

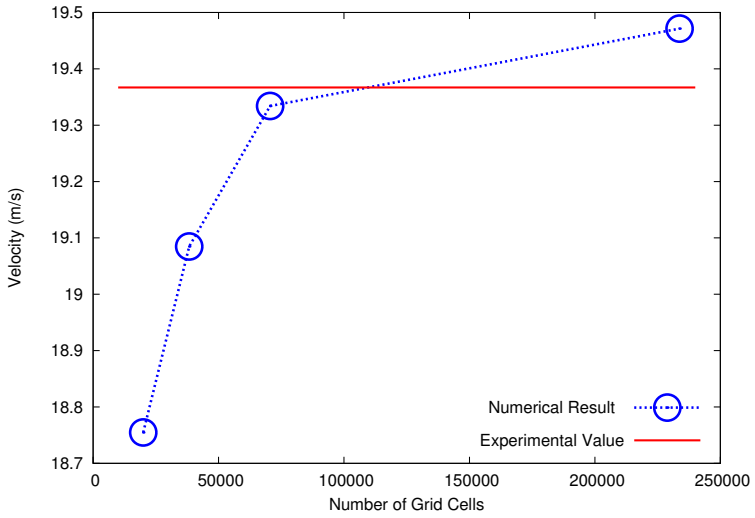

Figure 3: Computed centerline velocity at x/d=10 for each grid refinement compared with the experimental result.

more physically representative of the actual flow field, as the velocity is not assumed to be uniform across the jet exit.

Further analysis was performed for the case with the jet exit located at the disk trailing-edge to determine the sensitivity of the solution to changes in the jet turbulent inlet conditions. It was found that the solution was highly dependent on the inlet turbulence quantities, particularly the turbulent dissipation rate. The exact values of the turbulent quantities are not usually known for these experiments. A combination of inlet turbulence quantities was found that produced results similar to the case where the jet inlet was located upstream of the disk. However, unrealistic turbulence values were needed (i.e., a turbulent length scale on

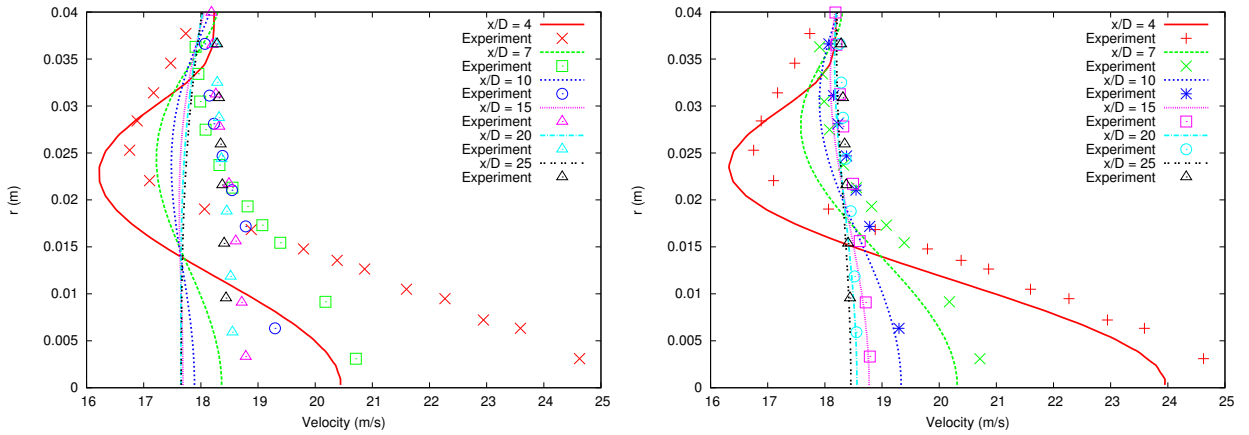

(a) Results with jet inlet located at the disk trailing-edge (b) Results with jet inlet located upstream of disk trailing-edge

Figure 4: Wake profiles at various locations downstream of the axisymmetric self-propelled disk.

the order of 10 meters).

Also, in Figure 4(b) it was observed that as the wake progresses downstream the computational solution more closely matches the experimental values. The centerline velocity and centerline TKE, in particular, are very closely approximated beyond 10 disk diameters downstream (see Figure 5). However, for each location, the experimental wake profile is more full than the computed profile. It appears that the turbulence model is underpredicting the wake diffusion due to shear, which is common for the $k-\epsilon$ turbulence model.

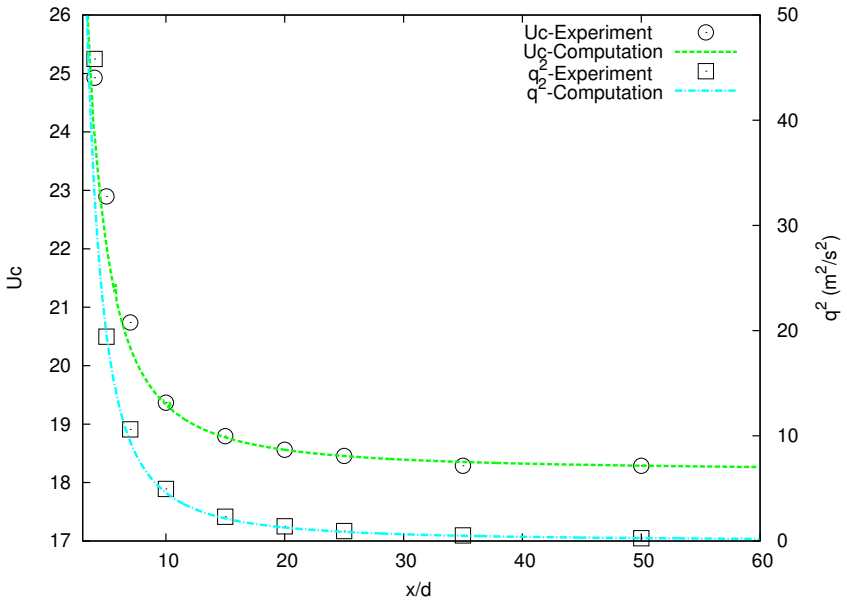

Figure 5: Normalized centerline defect velocity ($U_c = (\bar{u}_{centerline} - U_o)/U_o$) and centerline turbulent kinetic energy q^2 for the flow downstream of the axisymmetric self-propelled disk.

From this validation case it was determined that the $k-\epsilon$ model is capable of capturing the mean velocity and turbulent kinetic energy profiles with relatively good accuracy for locations beyond 10 diameters downstream. It was also found that the upstream jet supply channel must be included in the computational domain to correctly predict the turbulence characteristics at the jet exit. Neglecting the jet supply channel caused the solution to be highly dependent on the inlet turbulence quantities, which are not usually known.

4 Current Experiments with the GAMM Francis Turbine

4.1 Turbine Geometry

The GAMM Francis Turbine geometry [46] was used to evaluate the feasibility of adding a double-slot trailing-edge jet to a mixed flow hydroturbine. The GAMM Francis Turbine (see Figure 6) is a turbine model that was designed and tested by IMH-IMHEF-EPFL water turbine laboratory in Lausanne, Switzerland. The data for both the geometry and hydraulic performance are publicly available. The measurements were made in 1989 and were used for the 1993 GAMM Workshop on 3D Computation of Incompressible Internal Flows [47] in Lausanne. The GAMM Francis runner was also used in the annual ERCOFTAC Seminar and Workshop on Turbomachinery Flow Predictions [46].

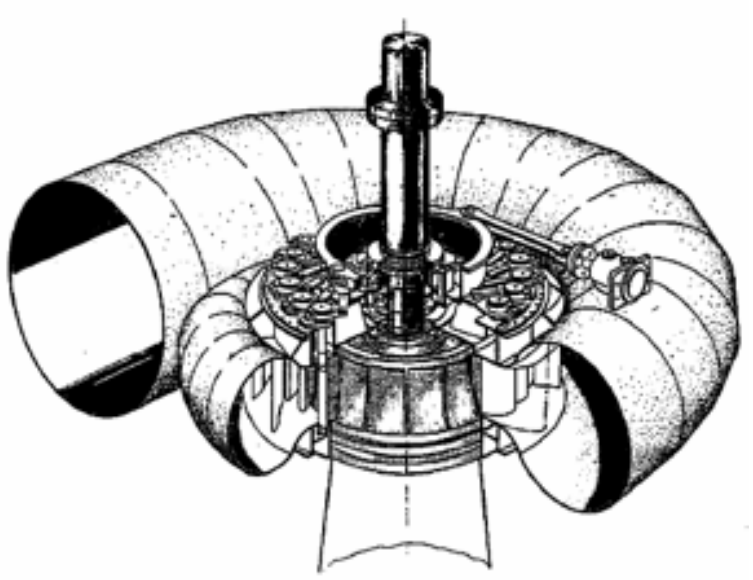

Figure 6: 3-D cut away of the GAMM Francis Turbine [46].

The specific speed of the GAMM Francis Turbine model is 0.5, with a runner diameter of 0.4 m, containing 13 runner blades. The distributor ring consists of 24 stay vanes and 24 wicket gates. Table 1 is a summary of the turbine performance characteristics when operating at the best efficiency point (BEP). All results presented here were obtained at BEP. Future work will focus on off-design operational conditions.

Table 1: Summary of the GAMM Francis Turbine operation at the best efficiency point.

Efficiency (%)	η	92
Flow Rate (m^3/s)	Q	0.372
Head (m)	H	5.98
Torque ($N-m$)	T	369.1
Speed (rad/s)	Ω	52.36

4.2 Guide Vane Jet Geometry

The chosen guide vane jet is a first attempt at a feasible method for including trailing-edge blowing from the guide vanes. The guide-vane-jet channel is composed of two thin slots equally spaced from the chord line of the guide vanes. Dual slots were chosen because Park and Cimbala [10] found that the two-slot configuration

outperformed the single-slot configuration and resulted in very rapid wake decay. The slots traverse the complete span of the guide vanes and are connected by narrow channels to a plenum located near the guide vane's pivot axis, as shown in Figure 7.

Figure 7: Geometry for the jet channels added to the guide vanes of the GAMM Francis Turbine.

As found in the validation case above, it was necessary to model the upstream jet supply channel to correctly predict the turbulence characteristics at the jet exit. Preliminary computations were performed with the GAMM geometry without modeling the jet supply channel. The solution demonstrated a high dependence on the inlet turbulence quantities and unrealistic turbulence values were needed to match the results obtained by modeling the jet supply channel.

5 Computational Considerations

Using OpenFOAM®, the flow through the turbine was modeled as 3-D incompressible steady turbulent flow. The continuity and Reynolds-averaged Navier-Stokes (RANS) equations were solved using a pressure-based SIMPLE approach (Semi-Implicit Method for Pressure-Linked Equations). To close the system of equations, the standard high Reynolds number $k - \epsilon$ turbulence model was used. To maintain numerical stability without sacrificing accuracy, a blended first-order and second-order advection scheme was applied. Under-relaxation was also applied to the momentum and turbulence equations to maintain stability while approaching the steady-state solution. The solution was considered converged when the solution residuals were reduced by at least three orders of magnitude.

As shown in Figure 8, only one periodic guide vane passage was analyzed. For simplicity, the runner blade was not included, only the flow passage and distributor vanes. As no moving runner was included in the domain, the computations were performed in the earth-fixed frame. The effect of the jet on the runner was evaluated by measuring the velocity at several locations where the leading edge of the runner passes through the guide vane wake.

5.1 Boundary Conditions

The domain inlet was located just upstream of the stay vanes. The radial and tangential velocities were specified to maintain the prescribed volume flow rate and average flow angle from the spiral case of 29° from tangential, as was recommended in the ERCOFTAC Seminar [46]. A more accurate approximation of the inlet condition solution would be obtained by modeling the penstock and spiral case distributor as well, but this geometry was not available. The inlet turbulence quantities were specified based on an assumed turbulent length scale of one-third the inlet height and 10% turbulence intensity. These values were recommended by Nilsson and Davidson [48].

The no-slip and impermeable conditions were applied to the velocity at all walls. Wall functions were used to model the turbulence quantities.

An artificial extension was added such that the outlet of the computational domain was located several meters downstream of the draft tube exit. At this location all parameters were constrained to a zero-gradient condition. This was a reasonable approximation, as very large computational cells were used to reach this location, and all fluctuations should be smoothed out through numerical diffusion.

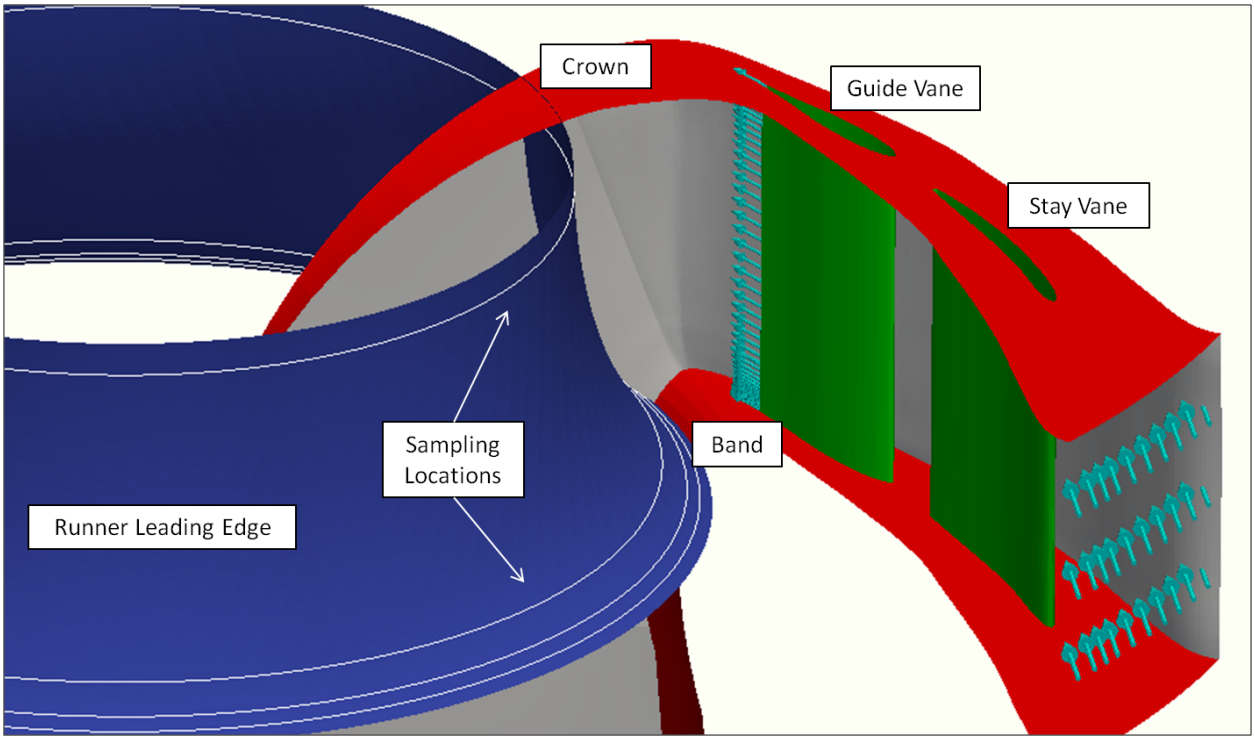

Figure 8: Isometric view of the flow through one periodic guide vane passage of the GAMM Francis Turbine. Also shown is the location of the leading edge of the runner blades and the four locations where flow data were sampled.

6 Results

6.1 Optimal Jet Flow Rate

The effect of the jet on the runner was evaluated by measuring the velocity at locations where the leading edge of the runner passes through the guide vane wake (these locations are shown in Figure 8). Jet flow rates ranging from 0.5% to 3% of the inlet volume flow rate were selected for evaluation. Velocity magnitude profiles for the various jet flow rates were compared to those of the non-jet case in Figure 9 at four locations along the span of the runner.

It is clear that blowing from the guide vane trailing-edge causes a reduction in wake deficit. The effect was most clearly observed at locations near the band, where the distance from the guide vane trailing-edge to the runner leading edge is the shortest. Due to the reduction in wake deficit, it is anticipated that the unsteady load variation observed by the runner will subsequently decrease. An unsteady simulation of the complete GAMM Francis turbine with and without guide vane trailing edge blowing is also being conducted by Lewis et al. [49]. The preliminary results indicate that the addition of blowing does decrease the unsteady load variation on the runner at the dominant blade passing frequencies.

The results shown in Figure 9 also indicate that the addition of blowing causes a significant global increase in mean velocity magnitude. A minor increase in velocity is to be expected due to the addition of mass to the system; however, for a 3% mass addition from the trailing-edge jet the average velocity magnitude increases by approximately 6%.

It was determined that the cause for the unexpected increase in velocity magnitude was an increase in swirl velocity. Due to the angle of the guide vanes, even a small amount of mass addition from the jets causes the swirl velocity to increase significantly, while the meridional velocity (the sum of the radial and axial velocities) increases proportionally to the mass addition. It is possible that this disproportionate increase in swirl may be utilized to adjust the average torque imparted to the runner blades without changing the guide vane opening angle or the turbine rotational speed. This will be be investigated in future research.

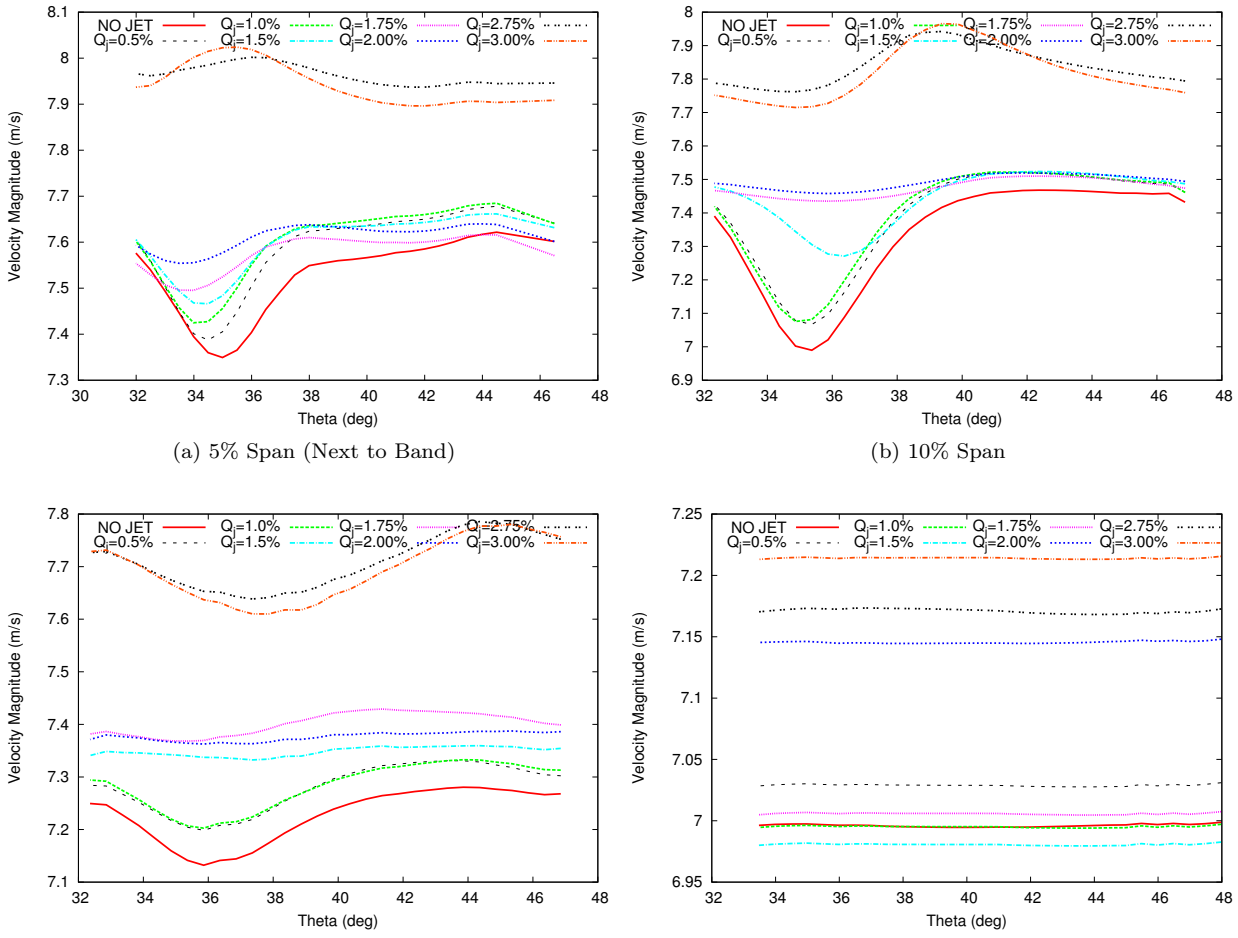

(a) 5% Span (Next to Band)

(b) 10% Span

(c) 20% Span

(d) 95% Span (Next to Crown)

Figure 9: Variation in wake profile due to the addition of blowing from the trailing-edge of the wicket gate observed at four locations on the runner leading edge.

It was also observed that the addition of blowing causes a circumferential shift in the wake location. This is another manifestation of the increased swirl caused by the blowing. The wake of the guide vane is displaced radially outward by the jet and does not reach the location of the runner leading edge until it has traveled a greater circumferential distance. However, this does not explain why the wake at 0% span (see Figure 9(a)) is displaced in the opposite direction. The cause for this discrepancy will be investigated in future research.

The final observation is that the wake from the guide vane was effectively diffused at locations near the crown without the addition of blowing (see Figure 9(d)). Therefore, no jet is needed in the upper section of the guide vane. Removing the jet from this area would not only reduce the required mass addition to the flow and the power to supply the jet, but it would also increase the structural stability of the guide vane as less material would need to be removed to create the jet channels. However, subsequent work by Lewis et al. [49] indicates that the wake in this region may also be decaying prematurely due to increased diffusion in the $k-\epsilon$ turbulence model when predicting swirling flows.

From the results shown in Figure 9 it was concluded that the optimal jet flow rate was between 1.75% and 2.0% of the inlet volume flow rate. A jet flow rate greater than 2% volume addition resulted in the wake profile transitioning to a jet profile, and a greater variation in velocity was observed. The conclusion agrees with findings by Waitz et al. [39], who recommend similar jet flow rates for axial turbofans.

6.2 Other Observations

A detailed examination of Figure 9(d) shows that for jet flow rates between 1% and 1.75% the average velocity magnitude for locations near the crown decreases, as opposed to the increase observed at all other locations along the runner. This behavior is more clearly shown in Figure 10, which presents the circumferentially averaged velocity at the runner leading edge, plotted as a function of percent span along the runner. For the above flow rate range, an axial shift in velocity distribution is observed. This may also be a result of the increased swirl. Increasing the swirl velocity results in higher angular momentum, which causes an outward displacement of the fluid mass. However, it has not yet been determined why this same phenomenon was not observed at higher jet flow rates. As no literature is available on trailing-edge blowing in mixed flow devices, such as Francis hydroturbines, this is an important topic for future research.

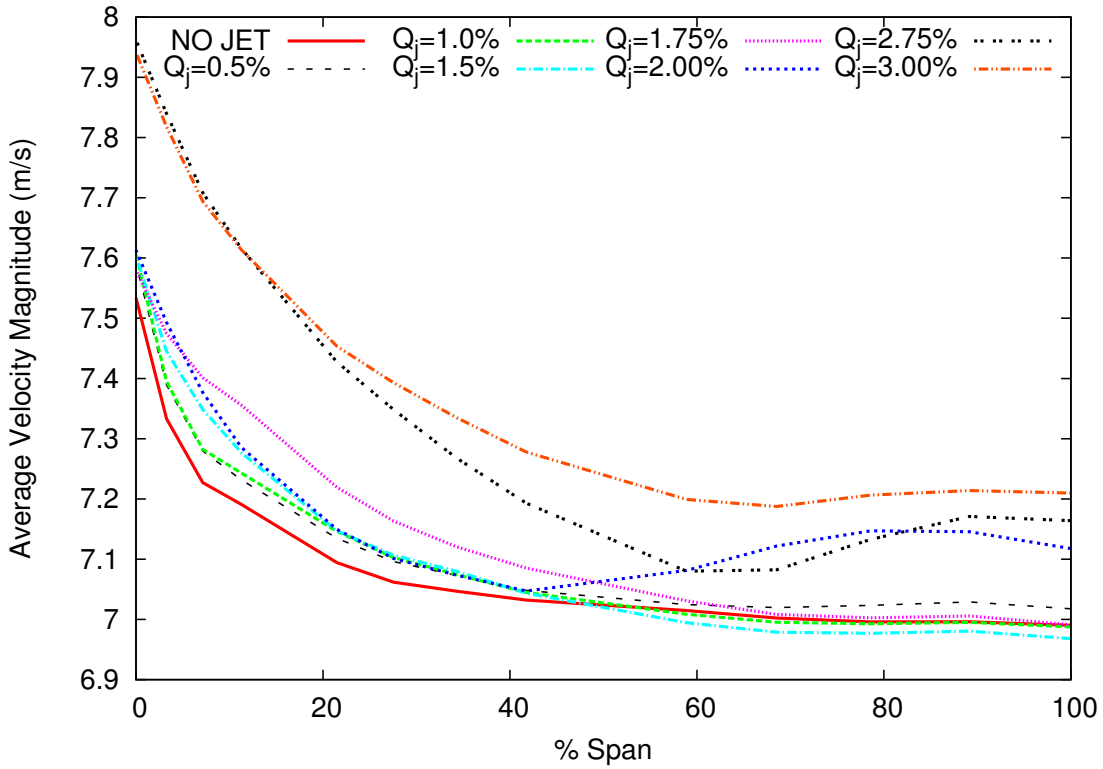

Figure 10: Circumferentially averaged velocity at the runner leading edge as a function of percent span along the runner blade, ranging from 0 at the band to 100 at the crown.

7 Conclusions and Future Work

A validation case using experiments by Naudascher [2] demonstrated the capability of the standard high Reynolds number $k-\epsilon$ turbulence model for simulations of momentumless wakes. It was found that the $k-\epsilon$ model sufficiently captures the mean velocity and turbulent kinetic energy profiles for locations beyond 10 diameters downstream. It was also found that the upstream jet supply channel must be included in the computational domain to correctly predict the turbulence characteristics at the jet exit. Neglecting the jet supply channel caused the solution to be highly dependent on the inlet turbulence quantities, which are not usually known.

Injection of water from the trailing-edge of the guide vanes is presented here as a method for reducing the unsteady load on hydroturbine runner blades. Reducing the unsteady load on runner blades would allow for leaner designs, smoother operation, and an increased lifespan of the hydroturbine. The flow through a single distributor vane passage of the GAMM Francis turbine was modeled at BEP for a range of jet flow rates

between 0.5% and 3% of the inlet volume flow rate. The effect of the jet on the runner was approximated by measuring the velocity at locations where the leading edge of the runner passes through the guide vane wake. The effect of the blowing was most clearly observed at locations near the band, where the distance from the guide vane trailing edge to the runner leading edge is the shortest. The optimal jet flow rate was found to be between 1.75% and 2% of the inlet flow rate. A jet flow rate greater than 2% volume addition resulted in the wake profile transitioning to a jet profile.

The results of the simulations also indicate that the addition of blowing causes a significant global increase in mean velocity magnitude and a circumferential shift in the wake location. For jet flow rates between 1% and 1.75%, an axial shift in velocity distribution was also observed. It appears that the increase in swirl due to the guide vane angle was the cause. However, no literature is available on trailing-edge blowing in mixed flow devices, and a more complete study of the correlation between the guide vane angle and the mean velocity magnitude is needed to validate this claim.

The final objective of this research is to understand the effects of guide vane blowing in order to improve hydroturbine performance at off-design conditions. Lewis et al. [49] are concurrently performing an unsteady CFD simulation of the complete GAMM Francis turbine with and without guide vane trailing edge blowing. The preliminary results indicate that the addition of blowing does decrease the unsteady load variation on the runner at the dominant blade passing frequencies. Future work will focus on mixed-flow conditions in which the wake of the guide vane more prominently interacts with the runner blade. This will allow for a more accurate prediction of the effects of guide vane blowing. An analysis of the effects of guide vane blowing at off-design conditions will then be conducted. Particular attention will be given to delaying the onset of extreme cavitation on the runner blades and the development of a draft tube vortex. The application of guide vane blowing to adjust the average torque imparted to the runner blades, without changing the guide vane opening angle or the turbine rotational speed, will also be investigated.

Acknowledgments

The authors would like to give special thanks to the Department of Defense High Performance Computing and Modernization Program for their generous donation of computational time and resources at their supercomputing centers. This research was made with government support under and awarded by DoD, Air Force Office of Scientific Research, and National Defense Science and Engineering Graduate (NDSEG) Fellowship, 32 CFR 168a. Partial support was also received from a DoE grant, Graduate Student Fellowship Program for Hydropower Research.

References

[1] M. Sick, W. Michler, T. Weiss, and H. Keck. Recent developments in the dynamic analysis of water turbines. *J. Power and Energy*, 223,A, 2009.

[2] E. Naudascher. Flow in the wake of a self-propelled body and related sources of turbulence. *J. Fluid Mech.*, 22:625–656, 1965.

[3] M. Ridjanovic. *Wake with zero change in momentum flux*. PhD thesis, University of Iowa, 1963.

[4] H. Wang. *Flow behind a point souce of turbulence*. PhD thesis, University of Iowa, 1965.

[5] A. I. Sirviente and V. C. Patel. Wake of a self-propelled body, part 1: Momentumless wake. *AIAA Journal*, 38(4):613–619, 2000.

[6] A. I. Sirviente and V. C. Patel. Wake of a self-propelled body, part 2: Momentumless wake with swirl. *AIAA Journal*, 38(4):620–627, 2000.

[7] G. G. Chernykh, A. G. Demenkovb, and V. A. Kostomakhac. Swirling turbulent wake behind a self-propelled body. *Int. J. Computational Fluid Dynamics*, 19(5):399–408, 2005.

[8] K. Brucker and S. Sarkar. A comparative study of self-propelled and towed wakes in a stratified fluid. *J. Fluid Mech.*, 652:373–404, 2010.

[9] J. M. Cimbala and W. J. Park. An experimental investigation of the turbulent structure in a 2D momentumless wake. *J. Fluid Mech.*, 213:479–509, 1990.

[10] W. J. Park and J. M. Cimbala. The effect of jet injection geometry on 2D momentumless wakes. *J. Fluid Mech.*, 224:29–47, 1991.

[11] R. S. Meyer and J. M. Cimbala. Suppression of the wake of a finite airfoil by trailing-edge blowing. *Bulletin of the American Physical Society*, 36(2664), 1991.
[12] T. Corcoran. Control of the wake from a simulated blade by trailing edge blowing. Master's thesis, Lehigh University, Department of Mechanical Engineering, 1991.
[13] R. G. Naumann. Control of the wake from a simulated blade by trailing edge blowing. Master's thesis, Lehigh University, Department of Mechanical Engineering, 1991.
[14] G. Birkhoff and E. H. Zarantonello. *Jets, Wakes, and Cavities*. Academic Press, 1957.
[15] H. Tennekes and J. L. Lumley. *A First Cource in Turbulance*. MIT Press, 1972.
[16] P. Diamessis, G. Spedding, and J. Domaradzki. Similarity scaling and vorticity structure in high-reynolds-number stably stratified turbulent wakes. *J. Fluid Mech.*, 671(1):52–95, 2011.
[17] A. S. Ginevskii, L. N. Ukhanovla, and K. A Pochkinka. Turbulent co-flows with zero excess momentum. *Fluid Mech. Soviet Res.*, 1(81-86), 1972.
[18] R. L. Gran. An experiment on the wake of a slender propeller-driven body. Rep.20086-6006- RU-00, June 1973, TRW Systems, 1973.
[19] D. R. S. Ko. A phenomenological model for the momentumless turbulent wake in a stratified medium. Rep. 20086-6007-RU-00, Apr. 1973, TRW Systems, 1973.
[20] J. A. Schetz and F. Stanley. Analysis of free turbulent mixing flows without a net momentum defect. *AIAA J.*, 10:1524–1526, 1972.
[21] T. Kubota. Turbulent wake behind a self-propelled body. Rep. GALCIT-138, California Inst. of Tech., 1975.
[22] R. C Swanson, J. A. Schetz, and A. K. Jakubowski. Turbulent wake behind slender bodies including self-propelled configurations. Vpi-aero-024, sept. 1974, Virginia Polytechnic Inst. and State University, 1974.
[23] S. Hassid. Collapse of turbulent wakes in stably stratified media. *J. Hydronautics*, 14:25–32, 1980.
[24] W. Park. *An experimental investigation of the turbulent structure in two-dimentional momentumless wakes*. PhD thesis, The Pennsylvania State University, 1989.
[25] J. W. Ahn and H. J. Sung. Prediction of two-dimensional momentumless wake by k - epsilon - gamma model. *AIAA Journal*, 33(4), 1995.
[26] J. R. Cho and M. K. Chung. A k - epsilon - gamma equation turbulent model. *J. Fluid Mech.*, 237:301–322, 1992.
[27] W. S. Lewellen, M. Teske, and C. P. Donaldson. Application of turbulence model equations to axisymmetric wakes. AIAA Paper 73-648, 1973.
[28] W. S. Lewellen, M. Teske, and C. P. Donaldson. Turbulent wakes in a stratified fluid. Rep. 226, Aug. 1974, Aero Res. Associates of Princeton, 1974.
[29] M. L. Finson. Similarity behavior of momentumless turbulent wakes. *J. Fluid Mech.*, 71:465–479, 1975.
[30] V. K. Shashmin. Hydrodynamics and heat exchange in turbulent momentumless wakes. *Eng. Phys.*, 44(438-442), 1983.
[31] V. I. Korboko and V. K. Shashmin. Dynamics and heat transfer of a turbulent and laminar momentumless wake. *Heat Transfer Soviet Res.*, 17(96-103), 1985.
[32] G. Chernykh and O. Voropayeva. Numerical modeling of momentumless turbulent wake dynamics in a linearly stratified medium. *Computers and Fluids*, 28(3):281–306, 1999.
[33] G. G. Chernykh and O. F. Voropaeva. Numerical models of the second and third orders for a momentumless turbulent wake dynamics in a linearly stratified medium. *Russian Journal of Numerical Analysis and Mathematical Modelling*, 23(6):539–549, 2008.
[34] P. Diamessis, J. Domaradzki, and J. Hesthaven. A spectral multidomain penalty method model for the simulation of high reynolds number localized incompressible stratified turbulence. *J. Compuational Physics*, 202(1):298–322, 2005.
[35] S. A. Orszag and Y. H. Pao. Numerical computation of turbulent shear flows. Flow Research Rep. 19, July 1973, Flow Research Inc., 1973.
[36] R. W. Metcalfe and J. J. Riley. Direct numerical simulations of turbulent shear flows. In *Proc. 7th Int. Conf. on Numerical Methods in Fluid Dynamics*, pages 279–284, 1987.
[37] T. A. Leitch, C. A. Saunders, and W. F. Ng. Reduction of unsteady stator-rotor interaction using trailing edge blowing. *J. Sound and Vibration*, 235(2):235–245, 2000.
[38] N. M. Rao, J. W. Feng, R. A. Burdisso, and W. F. Ng. Experimental demonstration of active flow

control to reduce unsteady stator-rotor interaction. *AIAA Journal*, 39(3):458–464, 2001.

[39] I. A. Waitz, J. M. Brookfield, J. Sell, and B. J. Hayden. Preliminary assessment of wake management strategies for reduction of turbomachinery fan noise. *J. Propulsion and Power*, 12(5):958–966, 1996.

[40] A. M. Wo, A. C. Lo, and W. C. Chang. Flow control via rotor trailing edge blowing in rotor/stator axial compressor. *J. Propulsion and Power*, 18(1):93–99, 2002.

[41] Y. D. Wu, X. C. Zhu, and Z. H. Du. Experimental investigation on momentumless wake and its application in reduction of unsteady stator-rotor interaction. New Trends in Fluid Mechanics Research: Proceedings of the Fifth International Conference on Fluid Mechanics, 2007.

[42] U. S. Department of Energy. Report to Congress on the Potential Environmental Effects of Marine and Hydrokinetic Energy Technologies. [`http://www1.eere.energy.gov/water/pdfs/doe_eisa_633b.pdf`], 2009.

[43] D. L. Sutliff, D. L. Tweedt, E. B. Fite, and E. Envia. Low-speed fan noise reduction with trailing-edge blowing. *Int. J. Aeroacoustics*, 1(3):275–305, 2002.

[44] R. S. Meyer and J. M. Cimbala. The Reduction of Discrete Tone Noise Due to Blade Row Interaction in Turbomachinery by Trailing-Edge Blowing. *U. S. Navy J. of Underwater Acoustics*, 43(1):49–59, 1993.

[45] G. P Succi. System and method for suppression noise produced by rotors. United States Patent No. 5217349, 1993.

[46] E. Parkinson. Turbomachinery Workshop ERCOFTAC II, Test Case 8: Francis turbine. Technical report, 1995.

[47] G. Sottas and I. L. Ryhming. 3D-computation of incompressible internal flows. Proceedings of the GAMM Workshop, Lausanne, Switzerland, 1993.

[48] H. Nilsson and L. Davidson. Validations of CFD against detailed velocity and pressure measurements in water turbine runner flow. *Int. J. Numer. Meth. Fluids*, 41, 2003.

[49] B. J. Lewis, J. M. Cimbala, and A. M. Wouden. Investigation of Distributor Vane Jets to Decrease the Unsteady Load on Hydroturbine Runner Blades. In *Proc. 26th IAHR Symposium on Hydraulic Machinery and Systems*, number IAHRXXVI-121, 2012.